Diffusion and solubility of mineral oils through ethylene-vinyl acetate copolymer

Amar Bellili, Nicolas David, Bruno Vandame, Qingxiao Wang, Yannick Goutille, Emmanuel Richaud

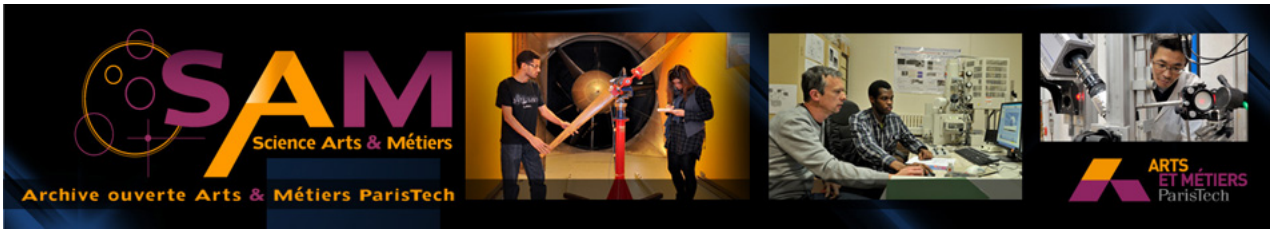

Property modelling

Diffusion and solubility of mineral oils through ethylene-vinyl acetate copolymer

Amar Bellili [a], Nicolas David [b], Bruno Vandame [b], Qingxiao Wang [b], Yannick Goutille [a], Emmanuel Richaud [b,*]

[a] Nexans Research Center, 29 rue pré Gaudry, 69353 Lyon Cedex, France
[b] Arts et Metiers ParisTech, CNRS, PIMM UMR 8006, 151 boulevard de l'Hôpital, 75013 Paris, France

Keywords:
EVA copolymer
Mineral oil
Diffusion
Solubility
Modelling
Activation energy

A B S T R A C T

This paper reports a study of mineral oil diffusion through a filled ethylene-vinyl acetate crosslinked polymer, together with some comparisons with aliphatic linear hydrocarbons. Permeation was monitored by classical gravimetric measurements leading to values of solubility and diffusion coefficient at several temperatures ranging from 20 to 120 °C. Diffusion coefficients display a change in activation energy at at ca. 70 °C for mineral oils but not for simple hydrocarbons. The values obtained were discussed regarding available structure-diffusivity relationships and diffusion models derived from free volume theory. A relationship between penetrant evaporation temperature and its diffusivity was observed and tentatively justified.

1. Introduction

Sorption and diffusion through polymeric matrices has aroused a considerable amount of literature for about fifty years [1]. Reliable models for describing diffusion kinetics are widely used in the case of Fickian diffusion [2] for describing the behaviour of "simple" binaries, as for example polyethylene and hexane [3], ethylene-vinyl acetate with various aromatic or aliphatic solvents [4].

Designing a truly predictive tool requires the assessment of diffusion coefficient whatever the temperature from the nature of polymer and penetrant. To that purpose, many theories have been proposed:

- Free volume theories according to which diffusion occurs through empty spaces continuously redistributed in the amorphous phase of polymer. The most elaborated theories can predict the cases in which solvent (or penentrant) brings its own free volume, thus autoaccelerating the diffusion process [5–8].
- Molecular models that are based on mathematical correlations between polymer type, stabilizer molar mass and temperature. They are generally designed for overestimation of D in cases of low diffusant concentration [9–14].

We have focused on the permeation of mineral oils though filled crosslinked ethylene vinyl acetate copolymer (EVA). Mineral oils are petrochemical by-products containing aliphatic, naphthenic and aromatic moieties, with linear or branched structures [15,16]. The diffusion of such complex fluids in polymers has been rarely reported [17,18], and this complexity is clearly a major issue for implementing some of the above mentioned models requiring the knowledge of a great number of polymer and oil parameters (WLF constant, T_g, specific volume of each elementary component…) [7,8].

* Corresponding author.
E-mail address: emmanuel.richaud@ensam.eu (E. Richaud).

This paper is hence aimed at:

- describing the permeation of complex fluids in a polymer,
- determining which laws can be applied to predict solubility and diffusion in EVA matrix despite the oil structural complexity, and which oil characteristic could be correlated (empirically or not) to its solubility and diffusivity in EVA.

2. Experimental

2.1. Materials

2.1.1. Polymer

The polymer matrix was a crosslinked ethylene vinyl acetate copolymer filled with aluminium hydroxide $Al(OH)_3$ (ATH). Residual Al_2O_3 weight value after a heating ramp up to 800 °C monitored by TGA was ca. 39% which corresponds to a total filler weight percentage close to 60%. Vinyl Acetate (VA) content was estimated from FTIR analysis using 3610/3460 cm^{-1} [19], 620/2680 cm^{-1}, 3460/2680 cm^{-1} and 1020/2680 cm^{-1} [20]. The three first ratios gave converging VA weight values ca. 20% whereas 1020/2680 cm^{-1} gave a significantly higher value (40%). Since the 1020 cm^{-1} absorption was calibrated only in the 2–6% VA weight range, we neglected this last result and considered that VA content was close to 20% in weight in the filler free matrix. Materials were supplied as 1 mm thick moulded plates from which various size samples (detailed latter) were cut.

DSC analysis (Fig. 1) revealed multiple melting endotherms at ca. 50, 70 and 115 °C with low transition enthalpy ($< 5\ J\ g^{-1}$) observed during the first heating scan but not for the second one, thus confirming the low ability of crosslinked polymers to crystallize from the molten state [21].

2.1.2. Mineral oil

n-dodecane (CAS number 112-40-3), n-hexadecane (CAS number 544-76-3) and icosane (CAS number112-95-8) were supplied by Sigma Aldrich. Their characteristics are given in Table 1. IRM 902 (density = 0.9346) and IRM 903 (density = 0.9206) correspond to the formerly called ASTM 2 and ASTM 3 oils. They were supplied by LRCCP (Vitry sur Seine – France). FTIR analysis (Table 2) allowed

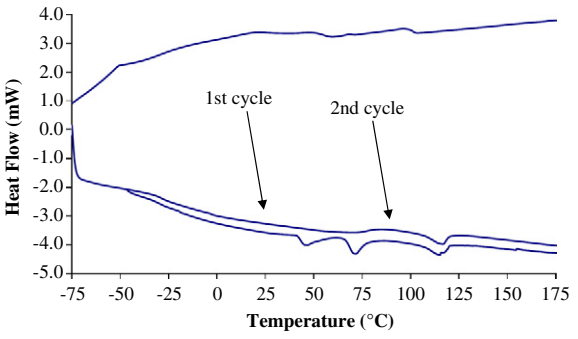

Fig. 1. Typical thermogram of EVA copolymer.

Table 1
Characteristics of hydrocarbons used as model oils.

Name	Formula	M (g mol^{-1})	T_m (K)	ΔH_m (J g^{-1})	T_b (K)
Dodecane	$C_{12}H_{26}$	170	264	228	487
Hexadecane	$C_{16}H_{34}$	226	293	210–236	543–561
Icosane	$C_{20}H_{44}$	282	309	218–251	616

percentages of paraffinic carbons (C_P), naphthenic carbons (C_N) and aromatic carbons (C_A) to be estimated using Brandes equations [22] from:

- absorbance at 1610 cm^{-1} with a baseline between 1650 cm^{-1} and 1560 cm^{-1}:

$$C_A = 1.2 + 9.8 \times \frac{DO_{1610}}{e} \quad (1)$$

- absorbance at 720 cm^{-1} with an horizontal baseline at 675 cm^{-1}:

$$C_P = 29.9 + 6.6 \times \frac{DO_{720}}{e} \quad (2)$$

- and:

$$C_N = 100 - C_A - C_P \quad (3)$$

Since this paper is concerned with prediction of diffusion from oil physical properties, these oils were characterized by several properties (see below).

2.2. Characterization procedure

2.2.1. Gel permeation Chromatography

Oils were analysed using a Waters 717 + apparatus. Stationary phase was Styragel HR1 thermostated at 35 °C. Detection was performed by Waters 2414 Refractive Index ($T_{detector}$ = 40 °C). Samples were injected in THF (HPLC grade supplied by Carlo Erba) at 0.1 ml min^{-1} flow.

Chromatograms are presented in Fig. 2. Using a column calibration with several n-alkanes, number average molar mass was estimated as 340 and 220 g mol^{-1}, respectively, with a polydispersity index close to 1. Another calibration using some aromatic compounds with short alkyl substituents (ethylbenzene, styrene, divinylstyrene, 1,2 epoxy-3 phenoxypropane, and DER 332 which is a bisphenol A diglycidylether monomer) gave 460 and 410 g mol^{-1}. The ideal set of standards should be made of molecules having the same rigidity as investigated oils. Despite the approximation linked to the choice of a standard set, it is obvious

Table 2
Percentages in paraffinic carbons (C_P), naphthenic carbons (C_N) and aromatic carbons (C_A) for IRM 902 and IRM 903.

	DO_{1605}	C_A (%)	DO_{725}	C_P (%)	C_N (%)
IRM 902	0.116	12.6	0.217	44.2	43.2
IRM 903	0.127	13.7	0.149	39.7	46.6

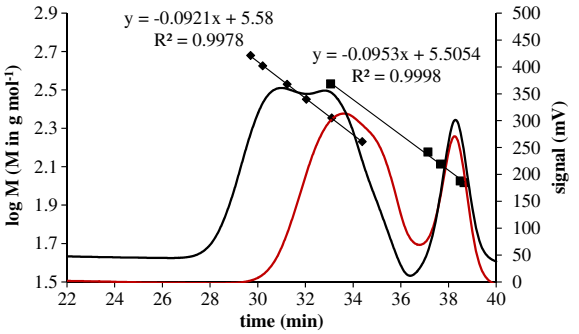

Fig. 2. GPC chromatograms of IRM 902 and IRM 903 oils (right axis) and calibration straights with n-alkanes (◆) and short substituents aromatic hydrocarbons (■).

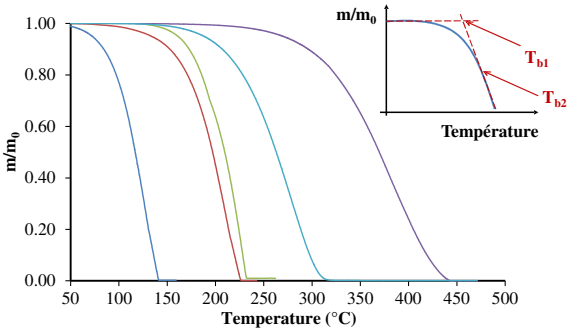

Fig. 4. ATG thermograms of hydrocarbons and mineral oil under study and graphical method for T_{b1} and T_{b2} onset temperatures.

that IRM 902 is made of bigger molecules than IRM 903. As will be seen later, molar mass of 460 for IRM 902 and 410 g mol^{-1} for IRM 903 are satisfying in a physical sense regarding diffusion kinetics and can be satisfactorily used as entry data for diffusion predictive models.

2.2.2. Differential Scanning Calorimetry

DSC experiments were carried out by subjecting samples of about 10 mg in closed aluminium pans to heating-cooling-heating cycles under nitrogen flow (50 ml min^{-1}). Apparatus was a Q10 DSC (TA Instruments) driven by Universal Analysis software.

Melting temperature and melting enthalpy of n-alkanes are gathered in Table 1. IRM 902 and IRM 903 cannot crystallize because of their structural complexity and display a transition characterized by a heat capacity jump (Fig. 3). This transition displays some common characteristics with glass transition temperature for a polymer. Note that it occurs about 40 °C below the pour point of each oil [23].

2.2.3. TGA Measurements

Oil evaporation temperature was characterized by TGA experiments under nitrogen (50 ml min^{-1}) using a TGA Q500 (TA Instruments) driven by Q Series Explorer: about 20 mg of oil was placed in a platinum pan and submitted to a 10 °C min^{-1} ramp from room temperature to 500 °C. Mass loss curves (Fig. 4) display a pseudo-sigmoidal shape from which onset temperatures were measured. T_{b1} and T_{b2} for model hydrocarbons and the mineral oils are reported in Table 3.

Table 3
Characteristic temperatures for mineral oils boiling.

	$C_{12}H_{26}$	$C_{16}H_{34}$	$C_{20}H_{42}$	IRM 902	IRM 903
T_{b1} (°C)	120	171	192	313	222
T_{b2} (°C)	145	198	212	371	263

2.2.4. Viscosity measurements

Measurements were conducted using an Ares rheometer (Rheometric Scientific) driven by TA Orchestrator software with a double wall Couette tool having the following geometry: inside cup diameter: 23.96 mm, inside bob diameter: 25.9 mm, outside bob diameter: 29.96 mm, outside cup diameter: 32.05 mm, bob length: 12.44 mm.

Samples were submitted to a dynamic pulsation sweep test from 10 to 100 rad s^{-1} at several temperatures from 25 to 120 °C, using 50% strain. It was first checked that this strain amplitude was in the linear viscoelasticity domain at each temperature. Viscosity measurements at various temperatures are given in Fig. 5 for a frequency sweep, and Fig. 6 for temperature sweep.

2.3. Exposure conditions

Exposures were performed according ISO 1817-2006 recommendations [24]. Polymer samples were cut as coarse rectangles corresponding well to the geometry allowing application of the mathematical solution of Fick's law proposed by Crank [2]. Some comparisons done with H2 specimens (width = 25 mm, total length = 75 mm, neck length = 25 mm) showed no significant deviation. Samples

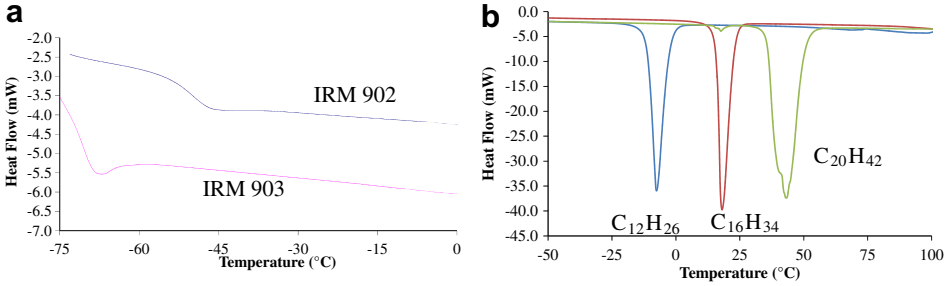

Fig. 3. DSC thermograms of IRM 902 and IRM 903 (a) and hydrocarbons used as model oils (b).

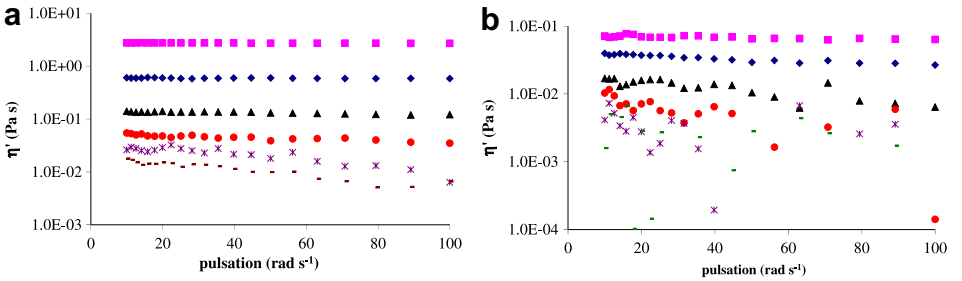

Fig. 5. Real component of viscosity measured at 25 °C (■), 40 °C (◆), 60 °C (▲), 80 °C (●), 100 °C (∗), et 120 °C (–) for IRM 902 (a) and IRM 903 (b).

of about 2 g were immersed in oil and regularly weighed until reaching maximal mass uptake. Excess liquid was removed from samples with clean paper before weighing, and after weighing they were re-immersed. Experiments were conducted in ventilated ovens or thermostated baths. Oil was thermally equilibrated for 24 h prior to exposure. It was checked by GPC that molar mass distribution of oil remained unchanged during the duration of permeation experiments and by FTIR whether any oil oxidation occurred.

3. Results

Kinetic curves for mass uptake were plotted for exposure at various temperatures ranging from 20 to 120 °C (Fig. 7). They display a classical shape including :

- An initial auto-slowing down increase,
- A plateau for long exposure times corresponding to the solubility of oil in EVA,
- A final decrease is suspected in many cases which might be due to extraction of soluble material, e.g. antioxidants, processing aids, free short chains, from EVA.

Some comparisons were done between :

- H2 specimens and rectangles ones, without significant difference,
- a sample obtained by slow cooling the crosslinked matrix (the industrial material) in water and the same material heated to 150 °C and dropped into liquid nitrogen in order to quench it. This comparison was aimed at highlighting the well-known influence of crystalisation on diffusion [25,26]. No significant effect was observed confirming the quasi-amorphous microstructure observed from DSC experiments (see Fig. 1).

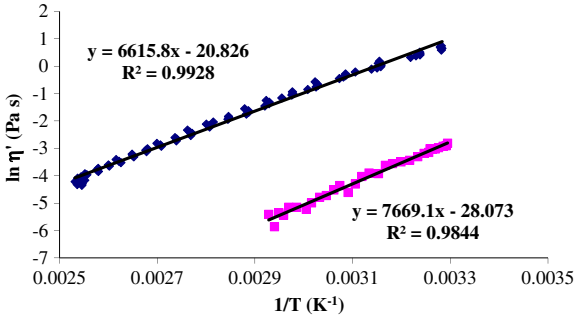

Fig. 6. Arrhenius plot of IRM 902 (◆) and IRM 903 (■) viscosity.

Whatever the temperature, it is clear that :

- Rates of permeation for oils are systematically ranked in the following order: $C_{12}H_{26} > C_{16}H_{34} > C_{20}H_{42} >>$ IRM 903 > IRM 902, in good agreement with the molar mass of the compounds.
- The maximal mass uptake order is : IRM 903 > IRM 902 > $C_{12}H_{26}$ > $C_{16}H_{34}$ > $C_{20}H_{42}$, even if solubility limits are generally very close for the three linear hydrocarbons under study, which is not surprising as will be seen later.

The diffusion mechanism can be characterized by plotting the mass uptake versus time on a log–log diagram. Mass uptake actually changes with time according the following power law:

$$\frac{m(t) - m_0}{m_\infty - m_0} = k \cdot t^n \tag{4}$$

m_0 and m_∞ being, respectively, the initial sample mass and the maximal value at the plateau, and m(t) the mass after immersion for time t. The exponent n was determined for various oil–temperature pairs (Fig. 8).

Let us recall that:

- If $n = ½$ for Fickian diffusion (case I), which corresponds to low polymer relaxation time compared to characteristic diffusion ones,
- If $n = 1$ for a non Fickian diffusion (case II), which corresponds to very high polymer relaxation times compared to characteristic diffusion ones,
- If n lies in between ½ and 1, diffusion is called abnormal, which is the most encountered situation in practice. Nevertheless, diffusion is considered as Fickian or non Fickian of n tends towards ½ or 1, respectively.

In fact, according to Hansen [27], case II would also correspond to Fickian diffusion with some particular conditions (low diffusion coefficient in the bulk compared to surface layer and slow interface crossing). Here, n is not too far from 0.5, so kinetics were assumed to be pseudo-Fickian as very often observed in elastomers [28,29]. Mass uptake is thus expected to obey the mathematical expression proposed by Crank in the case of an infinite plate both

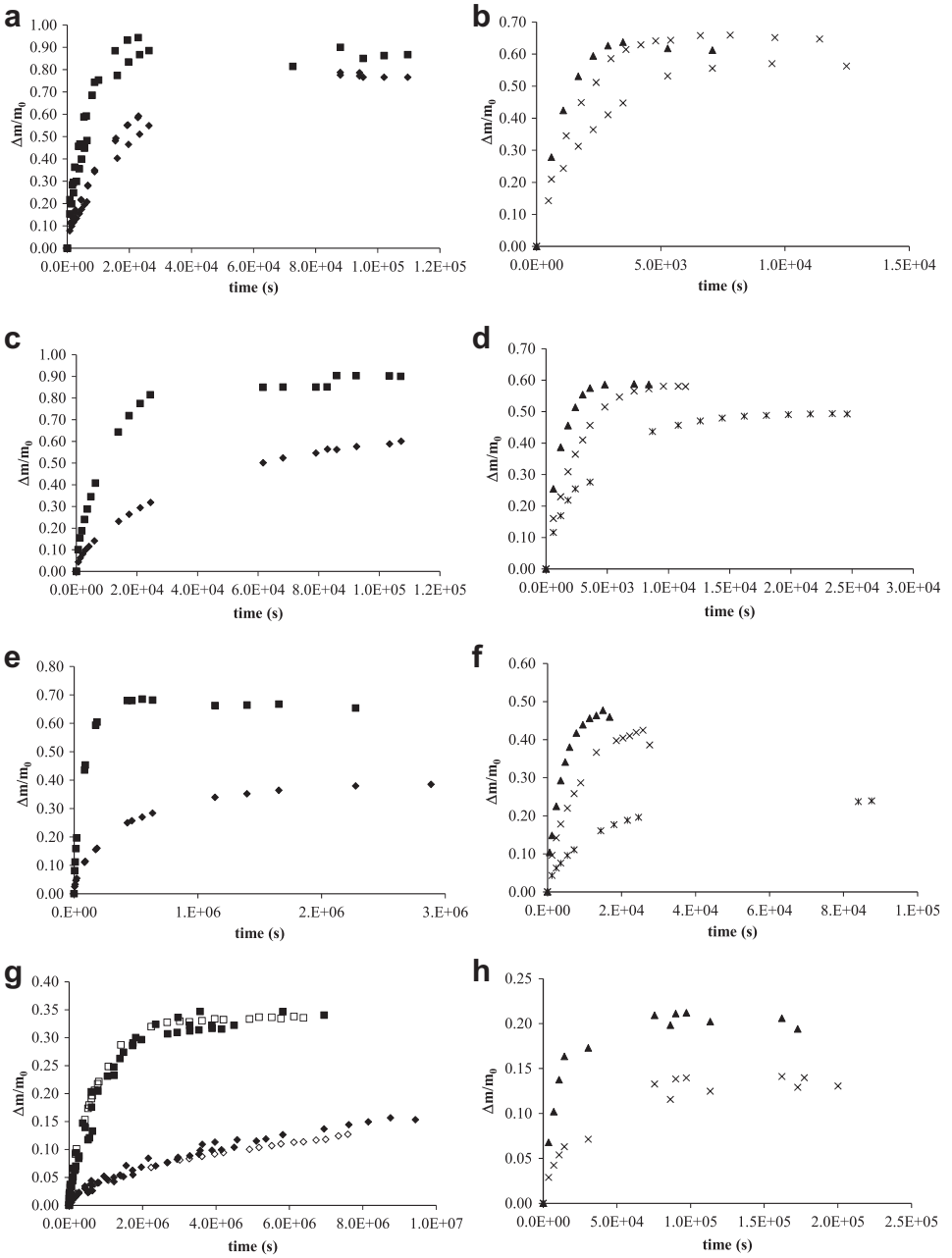

Fig. 7. Relative masse uptake of EVA immersed in IRM 902 (◆,◆), IRM 903 (■,□), $C_{12}H_{26}$ (▲), $C_{16}H_{34}$ (×), $C_{20}H_{42}$ (✱) at 120 °C (a, b), 90 °C (c, d), 50 °C (e, f) and room temperature (g, h). Open symbols correspond to quenched EVA.

sides of which are in contact with an infinite amount of penetrant [2]:

$$\frac{m(t)-m_0}{m_\infty-m_0}=1-\frac{8}{\pi^2}\cdot\sum_{i=0}^{\infty}\frac{1}{(2i+1)^2}\cdot\exp\left(-D\cdot(2i+1)^2\cdot\frac{\pi^2\cdot t}{e^2}\right) \tag{5}$$

which becomes when $(m(t) - m_0)/(m_\infty - m_0) < 0.6$:

$$\frac{m(t)-m_0}{m_\infty-m_0}=\frac{4}{e}\cdot\sqrt{\frac{D\cdot t}{\pi}} \tag{6}$$

e being the sample thickness. Diffusion coefficients were calculated from the slopes of $(m(t) - m_0)/(m_\infty - m_0)$ versus $t^{1/2}$ (corresponding figures are presented in the Appendix). Note that the linearity observed in the Figures also mitigates in favour of Fickian diffusion.

It has been proposed that the presence of fillers affects the diffusivity by increasing the tortuosity in the amorphous phase [26,30]. It is also noteworthy that the oil absorption provokes an increase in free volume and a subsequent diffusion autoacceleration (some models reporting a direct dependence of diffusion coefficient with

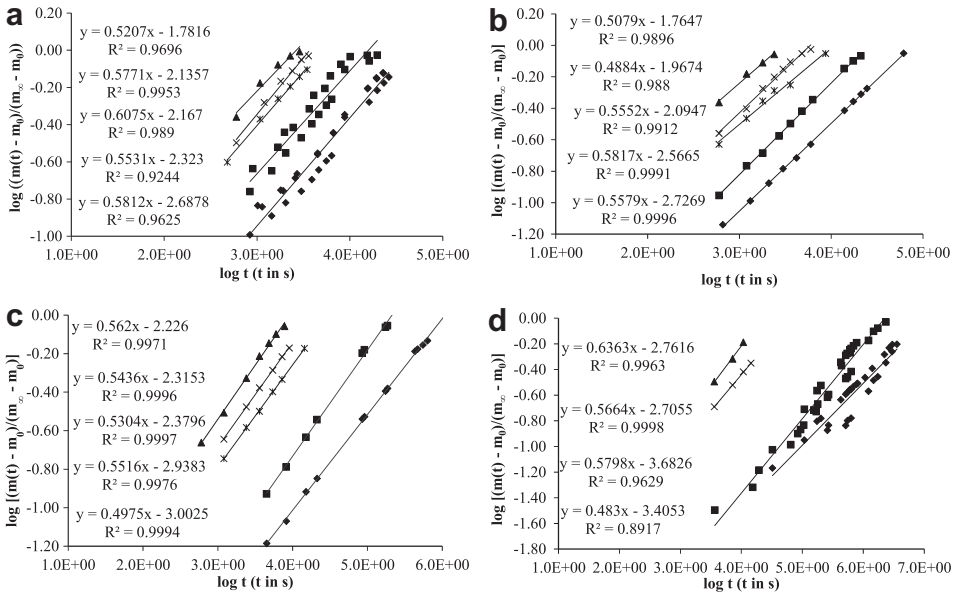

Fig. 8. Determination of diffusion mechanism for EVA immersed IRM 902 (◆), IRM 903 (■), $C_{12}H_{26}$ (▲), $C_{16}H_{34}$ (×), $C_{20}H_{42}$ (∗) at 120 °C (a), 90 °C (b), 50 °C (c) and room temperature (d).

penetrant concentration [26]) up to a plateau at high penetrant concentration [31]. Here, D will be considered as an apparent, average coefficient as many authors did in comparable cases [28,29,32,33]. The corresponding average values are given in Table 4. These values are plotted on an Arrhenius diagram (Fig. 9).

- For $C_{12}H_{26}$, $C_{16}H_{34}$, $C_{20}H_{42}$, D obeys the Arrhenius law within the experimental uncertainty. The activation energy is ca. 30 kJ mol^{-1} which corresponds well to the reported values of common aliphatic and aromatic values deduced from experimental results in several semi-crystalline thermoplastics having their amorphous phase in a rubbery state [32,33].
- For IRM 902 and IRM 903, a clear transition is observed at ca 65 °C at which E_D decreases from 70 to about 30 kJ mol^{-1} (i.e. the same value as for $C_{12}H_{26}$, $C_{16}H_{34}$ and $C_{20}H_{42}$).

It can be noted that for molar mass ranging between 100 and 1000 g mol^{-1} (which is certainly the molar mass range for oils under study), activation energies are generally between 20 and 100 kJ mol^{-1} [34], as observed here.

Viscosities were measured at several temperatures at a 100 rad s^{-1} angular rate for a 50% strain. They were plotted versus the corresponding diffusion coefficient in EVA (Fig. 10). This confirms that viscosity and diffusion coefficient are closely linked [35]. Assuming first that both viscosity and diffusion coefficient obey the Arrhenius law:

$$\ln\eta = \ln\eta_0 - \frac{\Delta H_\eta}{RT} \tag{7}$$

$$\ln D = \ln D_0 - \frac{\Delta H_D}{RT} \tag{8}$$

Exploitation of some previously published investigation of ester diffusion into chlorosulfonated polyethylene [36] suggested that D was inversely proportional to viscosity. Here, this is verified by results presented in Fig. 9 showing that $\Delta H_\eta \sim -\Delta H_D$, which will be discussed below.

Table 4
Average diffusion coefficients for $C_{12}H_{26}$ (▲), $C_{16}H_{34}$ (×), $C_{20}H_{42}$ (∗), IRM 902 (◆) and IRM 903 (■) at several temperatures.

	$C_{12}H_{26}$	$C_{16}H_{34}$	$C_{20}H_{42}$	IRM 903	IRM 902
120 °C	1.13×10^{-6}	8.09×10^{-7}	4.42×10^{-7}	1.50×10^{-7}	4.93×10^{-8}
110 °C	–	–	–	1.94×10^{-7}	–
100 °C	–	–	–	1.75×10^{-7}	3.67×10^{-8}
90 °C	7.28×10^{-7}	4.19×10^{-7}	2.64×10^{-7}	8.64×10^{-8}	2.89×10^{-8}
80 °C	–	–	–	7.97×10^{-8}	–
70 °C	–	–	–	5.79×10^{-8}	1.17×10^{-8}
65 °C	4.84×10^{-7}	1.96×10^{-7}	1.14×10^{-7}	3.28×10^{-8}	4.19×10^{-9}
60 °C	–	–	–	2.85×10^{-8}	3.16×10^{-9}
50 °C	2.44×10^{-7}	1.12×10^{-7}	6.55×10^{-8}	1.07×10^{-8}	1.61×10^{-9}
40 °C	–	–	–	5.31×10^{-9}	1.04×10^{-9}
23 °C	1.29×10^{-7}	2.57×10^{-8}	–	8.83×10^{-10}	2.53×10^{-10}

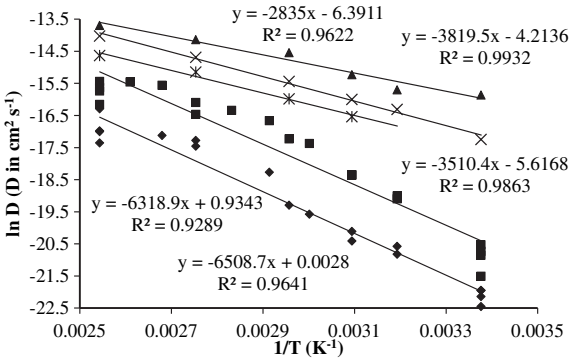

Fig. 9. Arrhenius diagram of diffusion coefficient for $C_{12}H_{26}$ (▲), $C_{16}H_{34}$ (×), $C_{20}H_{42}$ (∗), IRM 902 (◆) and IRM 903 (■).

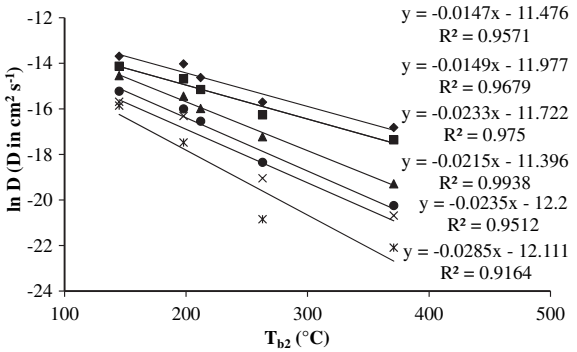

Fig. 11. Correlation between T_{onset} (see Fig. 3) and experimental D values (◆ :120 °C, ■ : 90 °C, ▲ :65 °C, ● :50 °C, × :40 °C, ∗ :23 °C).

Another correlation between diffusion coefficient of oil in EVA matrix and an oil property was found by plotting experimental D values versus T_{b1} and T_{b2} measured using TGA (see Experimental section). The most satisfying correlation is shown in Fig. 11.

Basically, in the case of IRM 902 and IRM 903, T_{b1} would correspond to the start of evaporation (certainly of the smallest molecules) and T_{b2} to the maximal evaporation rate (ie it would be characteristic of the greatest part of oil components) T_{b1} is undoubtedly correlated with boiling temperature [37], and it is assumed that it is also the case for the so-called T_{b2}. Note that Van Krevelen [38] proposed correlation between boiling temperature and solubility, but the correlation of the temperature with diffusion coefficient has not been reported to our knowledge. It will be tentatively justified in the Discussion section.

Even if oil uptake and extraction of soluble materials (uncrosslinked short chains, etc…) occurs during the mass uptake, the maximal mass uptake will be assumed to be equal to the solubility of oil in the polymer. Corresponding values are plotted in an Arrhenius diagram (Fig. 12). They display an obvious non-Arrhenian behavior contrarily to results obtained for the solubility of many hydrocarbons in elastomers [26,27].

4. Discussion

4.1. On the solubility limit

Considering first the case of aliphatic compounds studied as "model oils", ebullition temperatures are gathered in Table 1. According to Van Krevelen [38], these are correlated to the solubility coefficient by the equation:

$$\log sol(298) = -7.0 + 0.0123 \cdot T_b \tag{9}$$

$$10^{-3} \cdot \frac{\Delta H_S}{R} = 1,0 - 0,010 \cdot T_{LJ} \pm 0,5 \tag{10}$$

sol being expressed in m^3 (penetrant)/m^3 (polymer)/Pa, ΔH_S being expressed in J mol^{-1}, T_b and T_{LJ} in K. Then, the oil volume absorbed by polymer is calculated by Henry's law:

$$v_{oil}/v_{EVA} = sol \times P_{sat} \tag{11}$$

$$\log P_{sat} = A - \frac{B}{T + C} \tag{12}$$

Examples of calculation using Antoine's coefficient from relationships proposed by [39] are given in Table 5. The relative mass uptakes (ie the ratio of solubility for $C_{12}H_{26}$

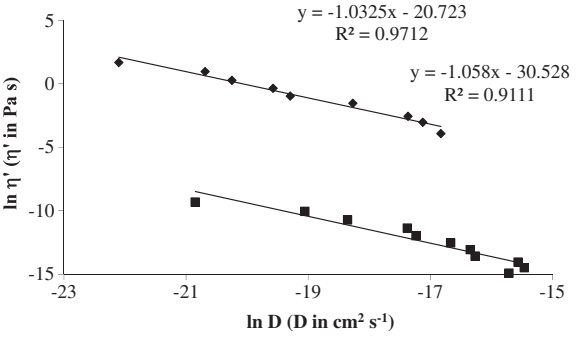

Fig. 10. Correlation between viscosity and diffusion coefficient for IRM 902 (◆) and IRM 903 (■).

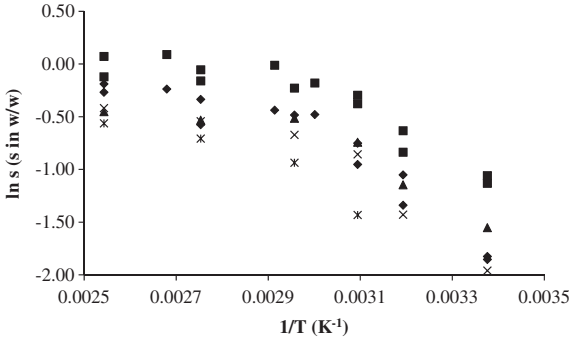

Fig. 12. Arrhenius plot of maximal mass uptake for $C_{12}H_{26}$ (▲), $C_{16}H_{34}$ (×), $C_{20}H_{42}$ (∗), IRM 902 (◆) and IRM 903 (■).

Table 5
Antoine coefficient for hydrocarbons used as model oils.

Name	S(298) in m^3STP/(m^3 Pa)	A	B	C	P_v (Pa)	v_{oil}/v_{EVA}
Dodecane	0.0977	6.7832	1557.55	185.28	26.90	2.63
Hexadecane	0.6160	6.8057	1762.24	170.14	0.64	0.39
Icosane	3.7740	6.8234	1963.77	155.25	0.01	0.03

and $C_{16}H_{34}$, and $C_{16}H_{34}$ and $C_{20}H_{42}$) are clearly not predicted so it can be concluded that this sort of correlation is not suitable for condensed phase.

The solubility of a pure liquid in a polymer can alternatively be expressed by the Flory-Rehner theory. However, for a highly filled matrix such as the EVA under study, fillers no doubt strongly affect Young's modulus. Assuming that the elastic response of swollen polymer is modified, there is no reason to use the Flory-Rehner equation to estimate solubility. It could be assumed that for complex mixtures, more sophisticated calculations for solubility prediction should be applied [40]. However, due to the moderate aromatic content for IRM 902 and IRM 903, and the relative similarity of aliphatic and naphthenic molecules, and neglecting also the certainly low moderate polar contribution of EVA acetate groups, the classical Flory's approach can be used for the cases under study:

$$\ln a_{oil}^{P} = \ln(1-\phi_{EVA}) + \left(1-\frac{V_{oil}}{V_{EVA}}\right)\phi_{EVA} + \chi\phi_{EVA}^{2} \tag{13}$$

where:

- a_{oil}^{P} is the oil activity in polymer,
- χ is the Flory–Huggins interaction parameter,
- ϕ_{EVA} volume fraction of polymer in swollen material (excluding the filler). In the case of a filled polymer, it was assessed by:

$$\phi_{EVA} = \frac{1}{1+\dfrac{w_{oil}}{1-w_{ATH}}.\dfrac{\rho_{EVA}}{\rho_{oil}}} \tag{14}$$

where:

- w_{oil} and w_{ATH} are, respectively, the weight ratio of oil in swollen matrix and the weight ratio of ATH in unswollen elastomer (i.e. $w_{ATH} = 0.65$)
- ρ_{EVA} is the pure EVA density (0.92), and ρ_1 the oil density.

At equilibrium, chemical potential of oil in polymer is equal to the chemical potential of pure oil: $a_1^{P} = a_1^{L} = 1$, so that, using the classical assumption for molar volume: $V_1 << V_2$

$$\chi = -\frac{\ln(1-\phi_{EVA}) + \phi_{EVA}}{\phi_{EVA}^{2}} \tag{15}$$

Using:

$$\chi = 0.34 + \frac{\overline{V}_{m_{oil}}}{RT}\cdot(\delta_{EVA}-\delta_{oil})^{2} \tag{16}$$

δ_{EVA} can be estimated from the oil uptake using $\delta_{C12H26} = 16.1$ MPa$^{1/2}$, $\delta_{C16H34} = 16.4$ MPa$^{1/2}$, $\delta_{C20H42} = 16.6$ MPa$^{1/2}$ [38]. δ_{EVA} was found in the range ca 18.0–18.5 MPa$^{1/2}$, in satisfying agreement with [41] for pure EVA, whereas EVA under study is about 60% filled. The choice of the entropic factor 0.34 is very often questioned but it leads here to the most satisfying solution. The two following conclusions arise:

- The filler has here a low effect on the solubility parameter of EVA,
- using Flory's equation with δ_{EVA} close to 18.3 MPa$^{1/2}$, solubility limits for linear hydrocarbons can be predicted with an accuracy systematically better than 80% which can be improved but constitutes a satisfactory method for predicting solubility of other hydrocarbons in EVA.

Some comparisons were also done with the results obtained by using the following equation proposed for semi-crystalline diffusant [42,43]:

$$-\frac{\Delta H_{m_{oil}}}{RT}\cdot\left(1-\frac{T}{T_{m_{oil}}}\right) = \ln(1-\phi_{EVA}) + \left(1-\frac{V_{oil}}{V_{EVA}}\right)\cdot\phi_{EVA} + \chi\cdot\phi_{EVA}^{2} \tag{17}$$

where $\Delta H_{m\ oil}$ and $T_{m\ oil}$ are, respectively, the melting enthalpy and temperature of oil expressed in J mol^{-1} and in K.

δ_{EVA} was found to increase with temperature from about 20 MPa$^{1/2}$ at room temperature to more than 28 at 120 °C, which is physically not reasonable since such a value exceeds the expected value for a polar polymer such as aliphatic polyamide. This means that, despite their ability to crystallize, the solubility of aliphatic compounds under study cannot be simulated by the precedent equation at temperatures above their melting point.

From the previously determined solubility parameter of EVA and the mass uptake value of IRM 902 and IRM 903, simple Flory's equation gave:

$$\delta_{IRM\ 902} \sim \delta_{IRM\ 903} \sim 17.0\ MPa^{1/2}$$

which is not surprising since IRM 902 and IRM 903 contain about 15% of aromatic moieties, these ones having a higher solubility parameter than aliphatic ones (for example 16.6 MPa$^{1/2}$ for cyclohexane versus 18.6 for benzene).

4.2. On the relation between viscosity and diffusion coefficient and on the arrhenian behavior of diffusion

Let us now try to explain why aliphatic compounds display a pseudo-Arrhenian diffusion coefficient but this is

obviously not the case for real mineral oils (Fig. 8). Let us recall that :

- no significant difference in D was observed for diffusion in EVA samples whether quenched or not (see Fig. 7),
- the breakdown in the Arrhenius diagram does not occur systematically for all oils.

The oil nature was suspected to be the most likely explanation for the deviation from the Arrhenius law.

Vrentas and Duda have modified the Cohen-Turnbull-Fujita theory to predict the diffusion coefficient value of solvent-polymer binaries within the whole range of concentration [1,7,8]. The general expression is:

$$D = D_{01}\cdot\exp\left(-\frac{E}{RT}\right)\cdot\exp\left(-\frac{\omega_1 V_1^* + \omega_2\xi V_2^*}{\dfrac{K_{11}\omega_1(K_{21}-T_{g1}+T)}{\gamma_1}+\dfrac{K_{12}\omega_2(K_{22}-T_{g2}+T)}{\gamma_2}}\right) \quad (18)$$

- E is the activation energy which is necessary to permit a solvent molecule jump, i.e. to overcome attractive forces and then diffuse,
- ω_1 and ω_2 are, respectively, weight ratio of oil and polymer,
- V_1^* and V_2^* are, respectively, solvent and polymer jumping unit specific volumes (here expressed in $cm^3\ g^{-1}$),
- ξ is the ratio of critical volume of solvent and polymer jumping unit,
- K_{11}/γ_1, K_{22}/γ_2 (in $cm^3\ g^{-1}\ K^{-1}$) and $K_{21} - T_{g1}$ and $K_{22} - T_{g2}$ (in K) are linked to WLF coefficients.

These parameters were determined for some polymers and some solvents including linear, cyclic aliphatic molecules and aromatic compounds. For example:

- K_{11}/γ_1 is on the order of 10^{-3} $cm^3\ g^{-1}\ K^{-1}$ for many common solvents,
- K_{12}/γ_2 is about a decade lower for polymers,
- $K_{22} - T_{g2}$ is on the order of -150 ± 25 K for elastomers such as PIB or EPDM (instead less than -300 for glassy polymers),
- $K_{21} - T_{g1}$ depends on penetrant structure and its value will be discussed here as the parameter responsible for linearity in the Arrhenius diagram.

Schematically, the temperature dependence of diffusion would be explained from simplifying the Vrentas and Duda equation:

$$\ln D = a - \frac{b}{K_{21} - T_{g1} + T} \quad (19)$$

Using many sets of V_1^*, V_2^* and ξ inspired from already published data [31,44–47], and the whole range of ω_1, $\omega_2 = 1 - \omega_1$, it is easy to verify that:

- If $|K_{21} - T_{g1}| << T$, changes of D with temperature roughly obey the Arrhenius law,
- when $|K_{21} - T_{g1}|$ increases (typically above 100 K), curvature appears.

$K_{21} - T_{g1}$ was reported of the order of -40 K for pentane and n-hexane. For cyclohexane (which is the simplest example of naphthenic compound), it falls to -160 K. Given the reported architectural complexity of mineral oil structure [15,16], lower values would be expected, thus explaining the difference between the pseudo-Arrhenius behaviour for $C_{12}H_{26}$, $C_{16}H_{34}$ and $C_{20}H_{42}$ and the non-Arrhenius behaviour for IRM 902 and IRM 903.

Oil viscosity is linked to its diffusivity from the free volume equation for pure solvent [48]:

$$\ln\left(\frac{0.124\times10^{-16}.\hat{V}_C^{2/3}\cdot RT\cdot d_1}{\eta_1.M_1}\right) = \ln D_{01} - \frac{\gamma.\hat{V}_1^*}{K_{11}.(K_{21}-T_{g1}+T)} \quad (20)$$

η_1, d_1, M_1 et V_{C1} being, respectively, the solvent viscosity, density, molar mass and critical volume. Hence: $\eta = aRT.D^{-1}$

Here also, it is easy to verify that changes of η with temperature lead to an activation energy that is nearly the opposite of that for diffusion. This is easily explained by the fact that changes of η with temperature depend mainly on change in D in the investigated temperature range and depend hardly at all on the changes of aRT.

4.3. On the prediction of diffusion coefficient from penetrant molar mass value

Despite the qualitative predictive power of the Vrentas and Duda free volume equation, this theory is in our mind too sophisticated to describe the diffusion of mineral oils under study in an industrial polymer because of the great number of parameters to be calculated for a “real” mineral oil.

We have, therefore, turned to molecular models as possible candidates for predicting D from oil characteristics and temperature. Several models [9–14] have been proposed for thermoplastic polymers having amorphous phase in a rubbery state and at solid state. They generally fit well the experimental data for linear molecules but discrepancies are expected for relatively complex structures, as for example mono- or polycyclic structures with side groups which is likely the case for IRM 902 and IRM 903 mineral oils [49].

We have here chosen the equation proposed by Brandsch, Mercea and Piringer [12] to try to predict diffusion coefficient value from temperature and penetrant molar mass. D actually varies quasi-linearly with $M^{2/3}$

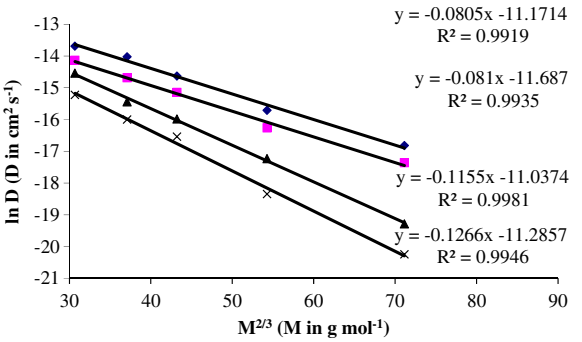

Fig. 13. Changes in diffusion coefficient of oils and n-alkanes at 120 °C (◆), 90 °C (■), 65 °C (▲) and 50 °C (×) versus molar mass.

(Fig. 13). According to experimental results, activation energy (or pseudo-activation energy in the case of IRM 902 and IRM 903) depends on penetrant molar mass, in good agreement with [34]. Here, it increases from 30 (for n-alkanes and IRM 902 and 903 at high temperature) to about 70 kJ mol^{-1} (for IRM 902 and 903 at low temperature).

For the sake of a simple predictive tool, it can be verified that the following empirical relation :

$$D = 10^4.exp\left(A - 0.11 \times M^{2/3} - \frac{E}{T}\right) \quad (21)$$

conveniently fits the obtained data with $A = -6.9$ and $E = 4600$ K.

There was the following alternative:

- Fix both E and A,
- Chose an activation energy depending on considered hydrocarbon, but the A constant was thus an adjustable parameter, which is not suitable for a predictive method.

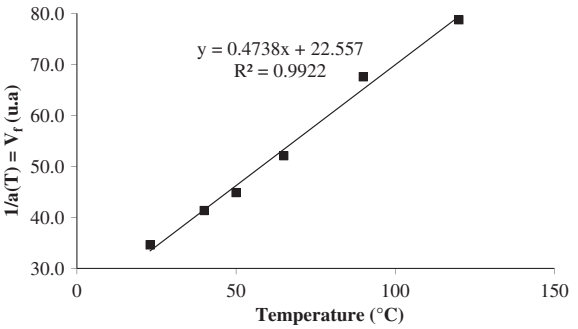

Fig. 15. Changes of $V_f(T) = 1/a(T)$ with temperature.

Despite being empirical, such a molecular model simulates roughly the diffusion in oil irrespectively of the role of structure complexity in diffusion [50] with a limited number of parameters. However, its mathematical structure does not permit simulation of the changes of diffusion coefficient temperature and other models have to be envisaged. More precisely, the model cannot take into account the free volume brought by the penetrant (as Vrentas and Duda theory does) which is the most possible explanation of its failure to satisfactorily simulate the temperature dependence of D.

4.4. On the correlation between diffusion coefficient and evaporation characteristic temperature

The existence of such a correlation is confirmed by reviewing data obtained for the diffusion of analogous or pseudo analogous series (differing by length of functional groups) of molecules into a given polymer matrix [33,36] (Fig. 14). This result would find its origin in the Cohen and Turnbull theory, according to which :

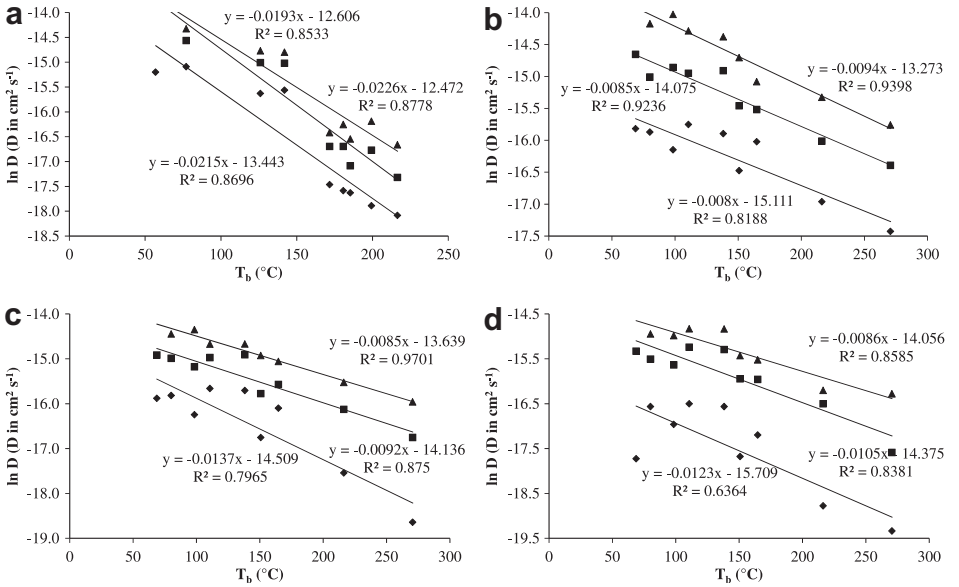

Fig. 14. Correlation of diffusion coefficient and boiling temperature. a: Esters in chlorosulfonated PE at 25 (◆), 50 °C (■), 60 °C (▲). b: Aliphatic and aromatic hydrocarbons in VLDPE at 25 (◆), 50 °C (■), 70 °C (▲). c: Aliphatic and aromatic hydrocarbons in LLDPE at 25 (◆), 50 °C (■), 70 °C (▲). d: Aliphatic and aromatic hydrocarbons in HDPE at 25 (◆), 50 °C (■), 70 °C (▲).

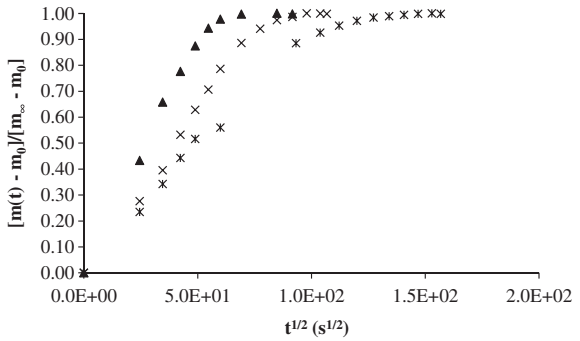

Fig. 16. Plot of $[m(t)-m_0]/[m_\infty-m_0]$ versus square root of time for EVA immersed in IRM 902 (◆,◆), IRM 903 (■,□), $C_{12}H_{26}$ (▲), $C_{16}H_{34}$ (×), $C_{20}H_{42}$ (∗) at 120 °C (a, b), 90 °C (c, d), 50 °C (e, f) and room temperature (g, h). Open symbols correspond to quenched EVA.

$$D = a\cdot\exp\left[-V^*/V_f(T)\right] \tag{22}$$

where:

- V_f is the free volume in polymer,
- V^* is the minimal size of a hole permitting the penetrant to move.

Thus:

$$V^* \,\alpha\, M \tag{23}$$

In a given chemical family, it is clear that:

$$T_b \,\alpha\, M \tag{24}$$

Note that the proportionality constant between V^* and M depends on the molecule flexibility, i.e. on the chemical family the molecule belongs to.

Finally, it is not surprising to find:

$$\ln D = \ln a - k\left(V_f(T)\right)^{-1}\cdot T_b \tag{25}$$

Then, the slope in Fig. 11 (denoted by a(T)) is inversely proportional to $V_f(T)$ which is related to the free volume in the polymer expressed by:

$$V_f = V_g + V_m\Delta\alpha\left(T - T_g\right) \tag{26}$$

The linear change of V_f with T (Fig. 15) militates in favor of this reasoning as well as data reported in Fig. 14.

5. Conclusions

This paper reports a study of diffusion and solubility of mineral oils and some linear hydrocarbons chosen as model systems in a filled and crosslinked EVA matrix. The diffusion regime was found to be Fickian within experimental uncertainty. Diffusion coefficients were thus calculated at several temperatures ranging from room temperature to 120 °C. In the case of linear hydrocarbons, they were found to obey the Arrhenius law while curvature was observed for IRM 902 and IRM 903 at temperature close to 60–70 °C. This curvature was tentatively explained using Vrentas and Duda free volume theory for diffusion. Due to the complexity of mineral oils and liquid environments to which the EVA is subjected in service conditions, simple tools should be proposed to predict diffusion kinetics of fluids into polymer. An empirical model linking molar mass temperature and diffusivity was proposed but failed to simulate the non arrhenian behavior of diffusion coefficient for mineral oils. Last, a correlation between diffusion and temperature characteristics of evaporation was proposed. This correlation was tentatively justified and seems to be applied to various cases of diffusion already reported in literature.

Appendix

Determination of diffusion coefficient from mass uptake curves (Fig. 16).

References

[1] L. Masaro, X.X. Zhu, Physical models of diffusion for polymer solutions, gels and solids, Prog. Polym. Sci. 24 (5) (1999) 731–775.
[2] J. Crank, The Mathematics of Diffusion. Clarendon Press, Oxford, 1975.
[3] B. Neway, M.S. Hedenqvist, V.B.F. Mathot, U.W. Gedde, Free volume and transport properties of heterogeneous poly(ethylene-co-octene)s, Polym 42 (12) (2001) 5307–5319.
[4] F.R. Perioto, M.E.T. Alvarez, W.A. Araujo, M.R. Wolf-Maciel, R. Maciel Filho, Development of a predictive model for polymer/solvent diffusion coefficient calculations, J. Appl. Polym. Sci. 110 (6) (2008) 3544–3551.
[5] M.H. Cohen, D. Turnbull, Molecular transport in liquids and glasses, J. Chem. Phys. 31 (5) (1959) 1164–1169.
[6] H. Fujita, Diffusion in polymer-diluent systems, Fortschritte Der Hochpolymeren-Forschung 3 (1) (1961) 1–47.
[7] J.S. Vrentas, J.L. Duda, Diffusion in polymer – Solvent systems - 1. Reexamination of the free volume theory, J. Polym. Sci. Polym. Phys. 15 (3) (1977) 403–416.
[8] J.S. Vrentas, J.L. Duda, Diffusion in polymer – Solvent systems - 2. A predictive theory for the dependence of diffusion coefficients on temperature, concentration and molecular weight, J. Polym. Sci. Polym. Phys. Ed. 15 (3) (1977) 417–439.
[9] E. Helmroth, C. Varekamp, Dekker. Stochastic modelling migration from polyolefins, J. Sci. Food Agr 85 (6) (2005) 909–916.
[10] E. Helmroth, R. Rijk, M. Dekker, W. Jongen, Predictive modelling of migration from packaging materials into food products for regulatory purposes, Trends Food Sci. Tech. 13 (3) (2002) 102–109.
[11] W. Limm, H.C. Hollifield, Modelling of additive diffusion in polyolefins, Food Addit Contam. 13 (8) (1996) 949–967.
[12] J. Brandsch, P. Mercea, O. Piringer, Modeling of additive diffusion coefficients in polyolefins. in: S.J. Risch (Ed.), Food Packaging Testing Methods and Applications, vol. 753. ACS Symposium Series, Washington DC, 2000, pp. 27–36.
[13] O. Piringer, Evaluation of plastics for food packaging, Food Addit Contam. 11 (2) (1994) 221–230.
[14] T. Begley, L. Castle, A. Feigenbaum, R. Franz, K. Hinrichs, T. Lickly, P. Mercea, M. Milana, A. O'Brien, S. Rebre, R. Rijk, O. Piringer, Evaluation of migration models that might be used in support of regulations for food-contact plastics, Food Addit Contam. 22 (1) (2005) 73–90.
[15] Leslie R. Rudnick (Ed.), Synthetics, Minerals Oils and Bio-Based Lubricants. Chemistry and Technology, CRC Taylor and Francis, Boca Raton New York London, 2006.
[16] F. Cataldo, Y. Keheyan, D. Heimann, A new model for the interpretation of the unidentified infrared bands (UIBS) of the diffuse interstellar medium and of the protoplanetary nebulae, Int. J. Astrobiology 1 (2) (2002) 79–86.
[17] A.B. Chai, A. Andriyana, E. Verron, M.R. Johan, A.S.M.A. Haseeb, Development of a compression test device for investigating interaction between diffusion of biodiesel and large deformation in rubber, Polym. Test. 30 (8) (2011) 867–875.
[18] G.M. Nasr, M.M. Badawy, Penetration of kerosene into carbon black-loaded SBR vulcanizates, Polym. Test. 15 (5) (1996) 477–484.
[19] G. Meszlényi, G. Körtvélyessi, Direct determination of vinyl acetate content in ethylene vinyl acetate copolymers in thick films by infrared spectroscopy, Polym. Test. 18 (7) (1999) 551–557.

[20] R.J. Koopmans, R. Van der Linden, E.F. Vansant, Characterization of newly developed and promising hydrolyzed ethylene vinyl acetate copolymers, J. Adhes. 11 (3) (1980) 191–202.
[21] E.S.A. Hegazy, T. Sasuga, T. Seguchi, Irradiation effects on aromatic polymers: 3. Changes in thermal properties by gamma irradiation, Polym 33 (14) (1992) 2911–2914.
[22] M.I.S. Sastry, A. Chopra, A.S. Sarpal, S.K. Jain, S.P. Srivastava, A.K. Bhatnaga, Carbon type analysis of hydrotreated and conventional lube-oil base stocks by i.r. spectroscopy, Fuel 75 (12) (1996) 1471–1475.
[23] http://www.univstrut.com/uploadfiles/pdf/5.pdf
[24] NFT ISO 1817-2006-11-01. Rubber, vulcanized – Determination of the effect of liquids.
[25] A.S. Michaels, H.J. Bixler, Flow of gases through polyethylene, J. Polym. Sci. 50 (154) (1961) 413–439.
[26] M. Hedenqvist, U.W. Gedde, Diffusion of small-molecule penetrants in semicrystalline polymers, Prog. Polym. Sci. 21 (2) (1996) 299–333.
[27] C.M. Hansen, The significance of the surface condition in solutions to the diffusion equation: explaining "anomalous" sigmoidal, Case II, and Super Case II absorption behavior, Eur. Polym. Jnl 46 (4) (2010) 651–662.
[28] S.C. George, S. Thomas, K.N. Ninan, Molecular transport of aromatic hydrocarbons through crosslinked styrene butadiene rubber membranes, Polym 37 (26) (1996) 5839–5848.
[29] A. Joseph, A.E. Mathai, S. Thomas, Sorption and diffusion of methyl substituted benzenes through cross-linked nitrile rubber/poly(ethylene-co-vinyl acetate) blend membranes, J. Membr. Sci. 220 (1–2) (2003) 13–30.
[30] L. Sereda, M. Mar López-González, L.L. Yuan Visconte, R.C.R. Nunes, C. Russi Guimarães Furtado, E. Riande, Influence of silica and black rice husk ash fillers on the diffusivity and solubility of gases in silicone rubbers, Polym 44 (10) (2003) 3085–3093.
[31] Q.L. Liu, H.Q. Gao, Prediction of mutual-diffusion coefficients in polymer solutions using a simple activity coefficient model, J. Membr. Sci. 214 (1) (2003) 131–142.
[32] T.M. Aminabhavi, H.G. Naik, Chemical compatibility testing of geomembranes - sorption/desorption, diffusion, permeation and swelling phenomena, Geotext Geomemb 16 (6) (1998) 333–354.
[33] T.M. Aminabhavi, H.G. Naik, Chemical compatibility study of geomembranes—sorption/desorption, diffusion and swelling phenomena, J. Hazard. Mater. 60 (2) (1998) 175–203.
[34] P. Dole, A. Feigenbaum, C. De La Cruz, S. Pastorelli, P. Paseiro, T. Hankemeier, Y. Voulzatis, S. Aucejo, P. Saillard, C. Papaspyrides, Typical diffusion behavior in packaging polymers application to functional barriers, Food Addit Contam. 23 (2) (2006) 202–211.
[35] E. Southern, A.G. Thomas, Diffusion of liquids in crosslinked rubbers. Part 1, Trans. Farad Soc. 63 (1967) 1913–1921.
[36] T.M. Aminabhavi, R.S. Munnolli, J. Dale Ortego, Interactions of chlorosulfonated polyethylene geomembranes with aliphatic esters: sorption and diffusion phenomena, Waste Manage. 15 (1) (1995) 69–78.
[37] J.W. Goodrum, Volatility and boiling points of biodiesel from vegetable oils and tallow, Biomass Bioenerg. 22 (3) (2002) 205–211.
[38] D.W. Van Krevelen, K. Te Nijenhuis, Properties of Polymers, Their Correlation with Chemical Structure; Their Numerical Estimation and Prediction from Additive Group Contributions, fourth ed. Elsevier, Amsterdam, 2009.
[39] K. Tochigi, M. Yamagishi, S. Ando, H. Matsuda, K. Kurihara, Prediction of Antoine constants using a group contribution method, Fluid Phase Equilibr 297 (2) (2010) 200–204.
[40] N. Vahdat, Solubility of binary liquid mixtures in polymeric materials, J. Appl. Polym. Sci. 50 (10) (1993) 1833–1839.
[41] P. Xu, Ethylene-vinyl acetate copolymer. in: J.E. Mark (Ed.), Polymer Data Handbook. Oxford University Press, Inc, New York, 1999, pp. 110–113.
[42] Y. Sun, J. Tao, G.G.Z. Zhang, L. Yu, Solubilities of crystalline drugs in polymers: an improved analytical method and comparison of solubilities of indomethacin and nifedipine in PVP, PVP/VA, PVAc, J. Pharm. Sci. 99 (9) (2010) 4023–4031.
[43] N.C. Billingham, in: H. Zweifel (Ed.), Plastics Additives Handbook, fifth ed. Hanser Gardner Publications, Cincinnati, 2001, p. 1019.
[44] M.P. Tonge, R.G. Gilbert, Testing free volume theory for penetrant diffusion in rubbery polymers, Polym 42 (4) (2001) 1393–1405.
[45] B.G. Wang, H.L. Lv, J.C. Yang, Estimation of solvent diffusion coefficient in amorphous polymers using the Sanchez–Lacombe equation-of-state, Chem. Eng. Sci. 62 (3) (2007) 775–782.
[46] J.S. Kim, K.R. Lee, Prediction of mutual diffusion coefficient in polymer solution, Polym 41 (2) (2000) 8441–8448.
[47] M.P. Tonge, R.G. Gilbert, Testing models for penetrant diffusion in glassy polymers, Polym 42 (2) (2001) 501–513.
[48] J.S. Vrentas, C.M. Vrentas, Predictive methods for self-diffusion and mutual diffusion coefficients in polymer–solvent systems, Euro Polym. Jnl 34 (5–6) (1998) 797–803.
[49] G. Bozzano, M. Dente, F. Carlucci, The effect of naphthenic components in the visbreaking modelling, Comput. Chem. Eng. 29 (6) (2005) 1439–1446.
[50] A. Reynier, P. Dole, S. Humbel, A. Feigenbaum, Diffusion coefficients of additives in polymers. I. Correlation with geometric parameters, J. Appl. Polym. Sci. 82 (10) (2001) 2422–2433.